# PROPULSION SIMULATOR FOR MAGNETICALLY SUSPENDED WIND TUNNEL MODELS

P.B. Joshi, M.R. Malonson, G.P. Sacco, and C.L. Goldey
Physical Sciences Inc.
Andover, MA

K. Garbutt and M. Goodyer
University of Southampton
England

and

P. Lawing
NASA Langley Research Center
Hampton, VA

## INTRODUCTION

Simulation of propulsion-induced aerodynamic forces and moments, which arise as a result of interactions between propulsive jets and the free stream, is one of the most desired capabilities in magnetic suspension wind tunnels. Such a simulation has always been a difficult task, even in conventional wind tunnels. The main reasons have been the problems of introducing high pressure air into the model, questions regarding proper scaling parameters, construction of models out of metric and non-metric sections, and accurately determining the force/moment contribution to the non-metric section.

Propulsion simulation for a magnetically suspended model presents special practical problems because there can be no physical connection between a compressed air reservoir and the model. Thus, propulsive gases must be generated on-board the model and then exhausted at desired locations on the model, Figure 1. The problem involves defining proper thrust (mass flow rate and velocity) requirements for the propulsive jet(s) and accomplishing gas generation within the volume of the model. Propulsion simulation in its entirety, whether for conventional or magnetically suspended models, involves both engine intake and exhaust jet flows. Only the latter is addressed in the work presented here. Our rationale is that the first step in simulation of propulsion should be to introduce the effects of the exhaust jet and that the complexities of allowing properly matched inlet flows should be deferred to later stages of development.

Under Phase I of an investigation sponsored by NASA LaRC, the feasibility of generating exhaust jets of appropriate characteristics on-board magnetically suspended models was examined. Four concepts of remotely operated propulsion simulators were considered. Three conceptual designs involving conventional technologies such as compressed gas cylinders, liquid monopropellants, and solid propellants were developed. The fourth concept, a laser-assisted thruster, which can potentially simulate both inlet and exhaust flows, was found to require very high power levels (tens of kilowatts). This concept

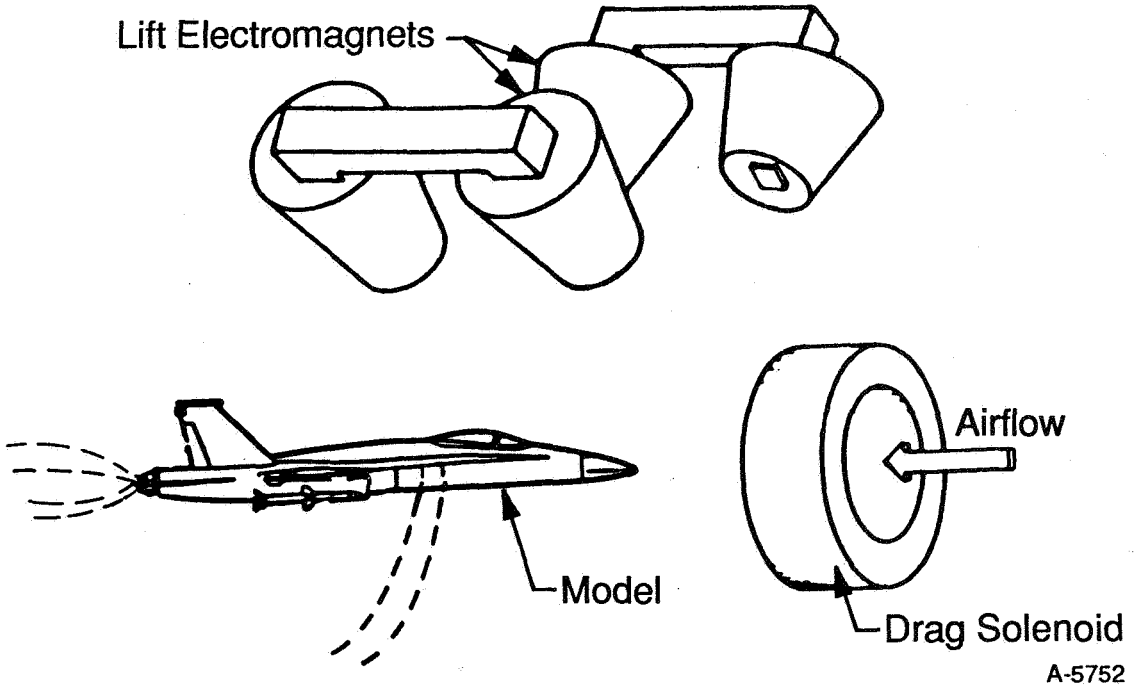


Figure 1. Schematic of Propulsion Simulation on a Magnetically Suspended Model

needs further research. The results of Phase I investigation, including a comparative evaluation of the four concepts, are discussed in Ref. 1.

The objective of current Phase II investigation sponsored by NASA LaRC was to demonstrate the measurement of aerodynamic forces/moments, including the effects of exhaust jets, in MSBS wind tunnels. Two propulsion simulator models were developed, a small-scale and a large-scale unit, both employing compressed, liquified carbon dioxide as propellant. The small-scale unit was designed, fabricated, and statically tested at Physical Sciences Inc. (PSI). It was tested in the 7-in. University of Southampton MSBS tunnel to measure forces/moments with jet on/off. The MSBS hardware and software were modified for this purpose to be compatible with the impulsive thrust forces associated with propulsive jets. The large-scale simulator was designed, fabricated, and statically tested at PSI.

This paper is in two parts. The first part presents design/development and static test data for the small-scale and large-scale simulators. The second part describes the modifications to the University of Southampton MSBS and results of the wind tunnel tests with the small-scale simulator. The paper concludes with recommendations for future developments including applications to conventional aeropropulsive testing.

# PART I

# PROPULSION SIMULATOR DEVELOPMENT

## 1. PROPULSION SIMULATOR DESIGN CONSIDERATIONS

Before describing the small-scale simulator, it is appropriate to discuss the design requirements. Since the existing MSBS wind tunnels (Ref. 2) allow the installation of relatively small models, a very limited volume is available for a propulsion device. Further, the magnetic core used for levitation also needs some space within the model, and the restrictions on the size of the propulsion simulator can indeed be significant. The largest operational MSBS wind tunnel in the U.S. at NASA LaRC has a 13-in. diameter test section. Another MSBS facility at University of Southampton, England, which is more versatile in that it has angle-of-attack variation capability, has only a 7-in. wide test section. In this wind tunnel, the model envelope would typically be 6 to 8-in. in length with 1 to 1.5-in. diameter centerbody. In the NASA tunnel, models 18-in. long by 3-in. diameter can be installed.

The design considerations are summarized in Table 1. The implementation of these requirements into the simulator design is discussed in Ref. 1.

The primary objective of the present work was to demonstrate the operation of a thrusting, propulsive model in an MSBS, and to measure the resulting forces/moments. The University of Southampton wind tunnel to be used for testing has a 7-in. octagonal test section. The small test section size and the desire to achieve high angles of attack ($\sim$45 deg), limits the model size. This limitation, in turn, restricts the number and the size of flow control components (a pressure regulator, an on/off solenoid valve, for example) that can be incorporated into the model. It was decided,

Table 1. General Design Considerations for Propulsion Simulators

| | |
|---|---|
| • Compactness | Smallest size possible for demonstration in current available MSBS tunnels |
| • High Density Propellant | Ability to carry the largest propellant mass in a given volume inside the model to maximize run time for a specified mass flow rate |
| • Relatively Lightweight | To minimize the size of magnetic core within the model and currents in external electromagnets |
| • Remote or Minimum Interference Activation | If remote activation is not feasible, the disturbance to flow field and magnetic field must be negligibly small |
| • Thrust Level | Compatible with particular MSBS capability |
| • Thrust versus Time Characteristics | Compatible with MSBS control system capability. Stable thrust duration must be sufficiently long so that data can be obtained after model becomes steady |
| • Safe Operation | Propellant material should be non-toxic, non-corrosive, with minimum of particulates |

therefore, to design and build two models: a small-scale simulator for demonstration in an MSBS and a large-scale simulator for static testing only. The small-scale model was developed principally to 1) demonstrate generation of an exhaust jet using $CO_2$ propellant, 2) guide in the design of the large-scale unit, and 3) verify the control and force/moment measurement of a thrusted model in the Southampton MSBS. The larger model was developed to 1) generate exhaust jets of desired characteristics; and 2) demonstrate the feasibility of propulsion simulation on larger wind tunnel models representative of practical applications.

The large-scale simulator was designed to generate a jet with pressure ratio, mass flow, and thrust requirements outlined in Ref. 1. This design permits intermittent, on/off operation of the jet. By contrast, the small-scale simulator was designed to be such that the propellant and some components must be replaced after every jet "run". No attempt was made to tailor the jet characteristics to the requirements of Appendix A for the small-scale device.

## 2. SMALL-SCALE PROPULSION SIMULATOR DESIGN

Figure 2 shows the small-scale simulator design which is a 1-1/8-in. diameter cylinder, 8-in. long, with hemispherical ends. The principal components are a 16g, liquified $CO_2$ cylinder (manufactured by Sparklet Devices), a cap-piercing hardened pin and squib mechanism (adapted from a design by Special Devices, Inc. (SDI)), battery and electronics assembly housed in the nose, three removable sets of copper spheres, and a nozzle. These components are housed inside a tube, 1/8-in. thick, made from an electromagnetic alloy formulated by Connecticut Metals, Inc. (CMI). The total weight of the simulator is about 600g with approximately 500g of magnetizable materials. The latter includes the material of the $CO_2$ cylinder and other miscellaneous components such as retainer rings, fasteners, spacers, etc. Figure 3 shows the distribution of the magnetizable mass in the simulator.

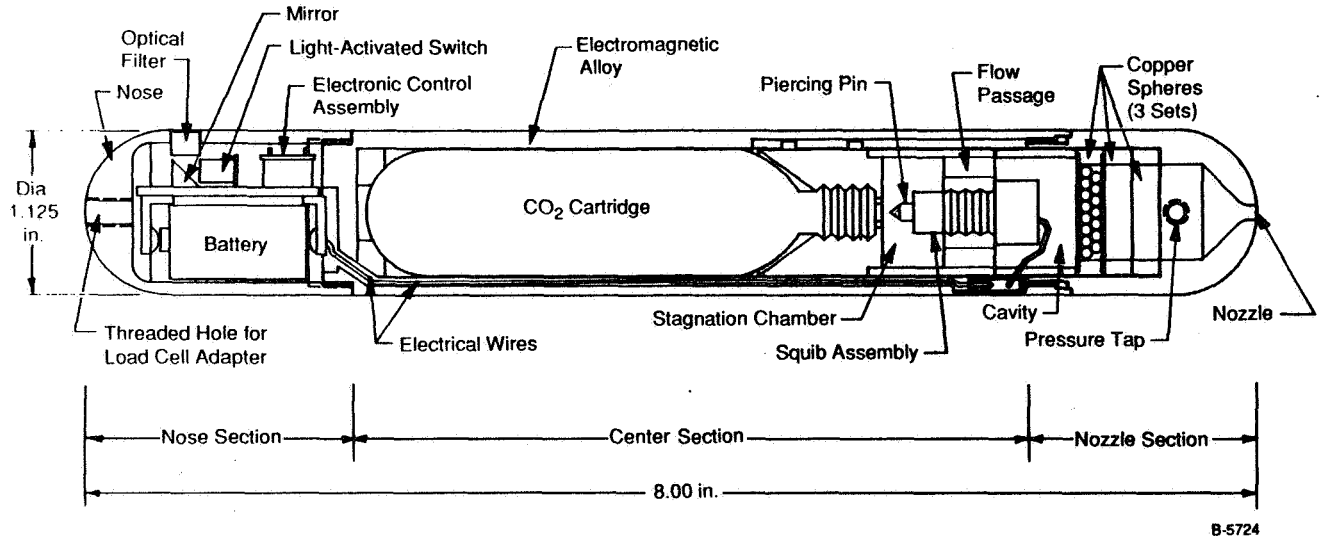


Figure 2. Small-Scale Propulsion Simulator Design

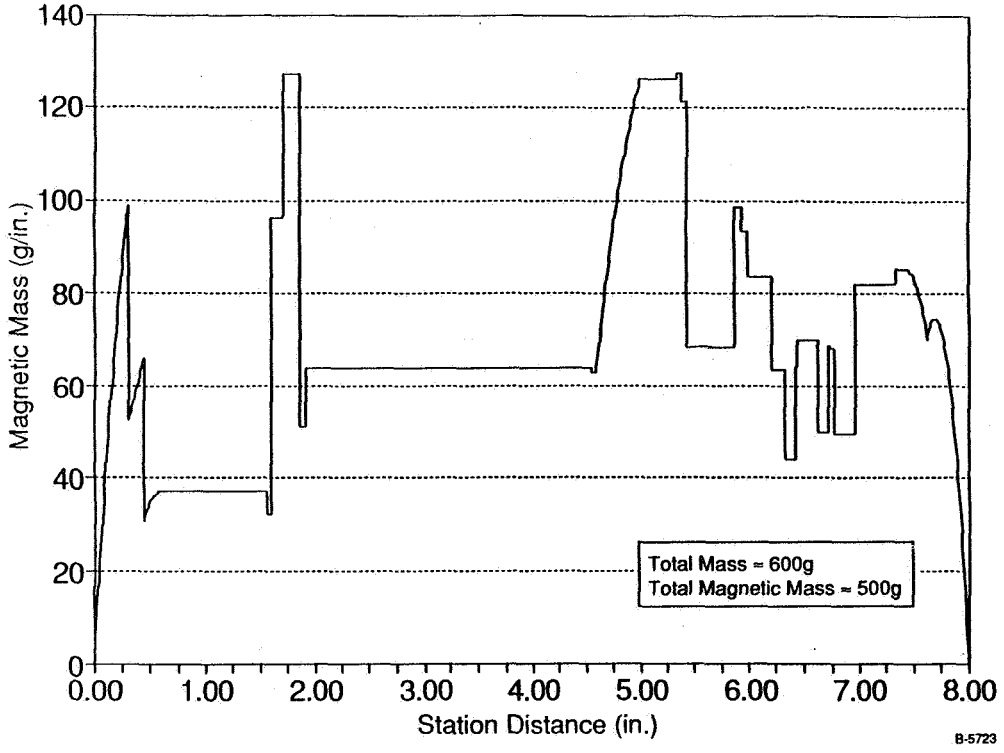


Figure 3. Magnetic Mass Distribution in the Small-Scale Simulator

The simulator consists of three major subassemblies: nose section, center section, and nozzle section. The nose section, which screws onto the center section, contains the battery (Kodak K28A) used as a power source for firing the squib (made by Cartridge Actuated Devices, Inc.) and the electronics assembly. The latter consists of a light-activated switch (EG&G, VTIC1110), a small mirror, and a silicon controlled rectifier, all mounted on a 0.06-in. thick circuit board. The battery is held inside a retaining clamp onto which the circuit board is mounted. An optical filter is embedded in the wall of the nose section. The filter allows HeNe laser wavelength (632.8 nm) to pass to the light activated switch. A pair of 22 AWG wires runs from the circuit board to the squib in the center section.

The center section of the simulator contains the $CO_2$ cartridge with its threaded neck screwed into a cylinder retainer which is held in place by a squib retainer. The pin-squib mechanism (made by SDI) is screwed into the threaded hole at the center of the squib retainer. The SDI design was modified such that inexpensive squibs made by Cartridge Actuated Devices could be incorporated into it. Had this modification not been done, the complete SDI pin/squib mechanism would have required replacement after each firing, costing about $150. Our design modification makes it possible to replace the squib only, for approximately $5 to $10. Earlier in the program, the "standard" piercing pin (also called "large" pin) in the SDI component was used. It had an internal hollow passage 0.050-in. diameter to draw $CO_2$ from the cylinder. Two holes, 0.050-in. diameter, in the 0.045-in. thick walls of the standard pin, expel the $CO_2$ into a stagnation chamber. The gas then flows from the chamber into a cavity surrounding the squib assembly through four oval passages drilled into the squib retainer. Another pin, with smaller outside and inside diameters, and with smaller ports for expelling $CO_2$, was also used during development. Both pins were case-hardened to ensure reliable penetration of the diaphragm of the $CO_2$ cylinder. Moreover, hardening also improved the usable life of the firing pin. Two holes (not shown in Figure 2) are drilled into the wall of the center section for measuring pressure in the stagnation chamber and in the cavity upstream of the nozzle section. The two 22 AWG wires

connecting the squib to the electronics in the nose section pass through a lengthwise groove machined in the wall of the center section.

The nozzle section screws onto the back end of the center section of the simulator. It contains three baffle assemblies which can be loaded with copper spheres of 1 or 2 mm diameter. Each assembly consists of a copper housing (a ring as shown in Figure 2) with a copper wire mesh at each end for retaining the spheres. Each assembly can be individually removed and replaced by a ring made of the CMI electromagnetic alloy. The purpose of the three copper plugs was to introduce a drop in total pressure as the $CO_2$ negotiated a tortuous path, and secondly, to vaporize any fine solid particles of $CO_2$ which may be present in the flow. As will be discussed later, the copper plugs were not always effective. A convergent passage was drilled into the nozzle with a baseline diameter of 0.098 in. A separate nozzle section with exit diameters of 0.298 in. was also used. Both nozzle sections were tested. The larger nozzle, used on a 1/40-scale model, corresponds to 12-in. full-scale throat diameter. A pressure tap was drilled into the nozzle wall downstream of the copper plugs and upstream of the exit orifice.

The operation of the small-scale simulator consists of shining a HeNe laser beam onto the optical filter in the nose section. The light switch is activated and the SCR then draws approximately 1 amp current from the battery to fire the squib. Explosion of the squib drives the pin (which moves against O-ring friction) into the diaphragm which caps the $CO_2$ cylinder. Only about 45 psi pressure is needed to rupture the diaphragm and the squib supplies 70 to 150 psi from the gaseous products of explosion. After penetration the pin stays in place due to the friction of the O-ring inside the housing of the SDI squib assembly. $CO_2$ liquid-gas mixture flows through the center passage in the pin and escapes through the two holes drilled in the walls (Figure 4). Upon passage through the squib retainer (Figure 5), the $CO_2$ flows through the copper plug(s) into the nozzle chamber and out through the orifice producing a jet.

## 3. RESULTS OF STATIC TESTING OF SMALL-SCALE SIMULATOR

The static tests were designed to yield thrust versus time history and pressure versus time history, the latter at three locations within the simulator. The thrust versus time data are necessary for design of the MSBS control system so that the model stays in place as it reacts to the propulsive jet turning on/off. The pressure data, which are diagnostic in nature, provide important insight into the effectiveness of the copper plug(s) in creating a pressure drop and into the gas dynamic processes within the simulator.

The schematic of the static-test set-up is shown in Figure 4. A load cell manufactured by Sensotec was used to obtain force (i.e., thrust) data. The pressure transducers were supplied by D.J. Industries and located as shown in Figure 4(b). The pressure $P_2$ and $P_1$ give a measure of the effectiveness of the copper spheres in creating a pressure drop. The pressures $P_2$ and $P_3$ give a measure of the gas dynamic processes and losses due to jet impingement on the cylindrical walls of the simulator. The load cell and transducer signals were sampled at 1 kHz. Visual observations of the jet just outside the nozzle exit plane indicated whether or not mist was present. The presence of mist shows that the copper spheres were not very effective in vaporizing the tiny solid particles formed during the expansion of $CO_2$ from compressed liquid to vapor.

Selected data from the simulator tests are presented in Figures 5 through 8. Each figure contains thrust and pressure versus time history. The three pressures, $P_1$, $P_2$, and $P_3$ are given on the same plot. Appendix B contains the small-scale simulator test matrix.

Figure 5 shows thrust and pressure curves for the baseline simulator configuration without any copper plugs. After an initial spike which reaches 4 lbf, the thrust rises to a maximum of about 1.9 lbf in about 0.1s and decreases gradually over the next 1.2s. An average thrust of about 1 lbf over a duration of 0.5s is achieved. The rise in thrust is due to the increase of pressure as the $CO_2$ fills up the simulator volume. The fall in thrust thereafter is directly due to the dropping stagnation pressure inside the simulator as the $CO_2$

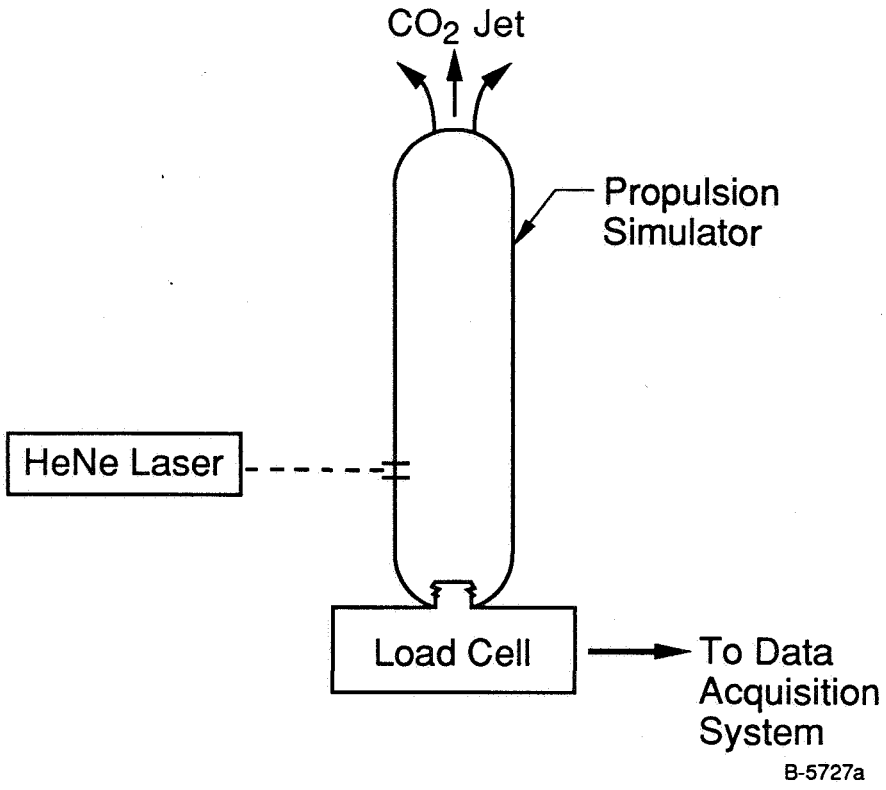


(a) Thrust Measurements

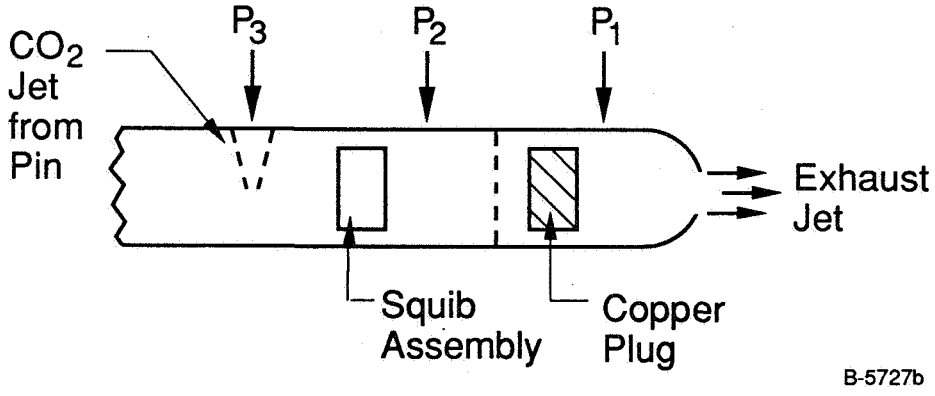


(b) Pressure Measurement

Figure 4. Schematic of Small-Scale Simulator Static Testing

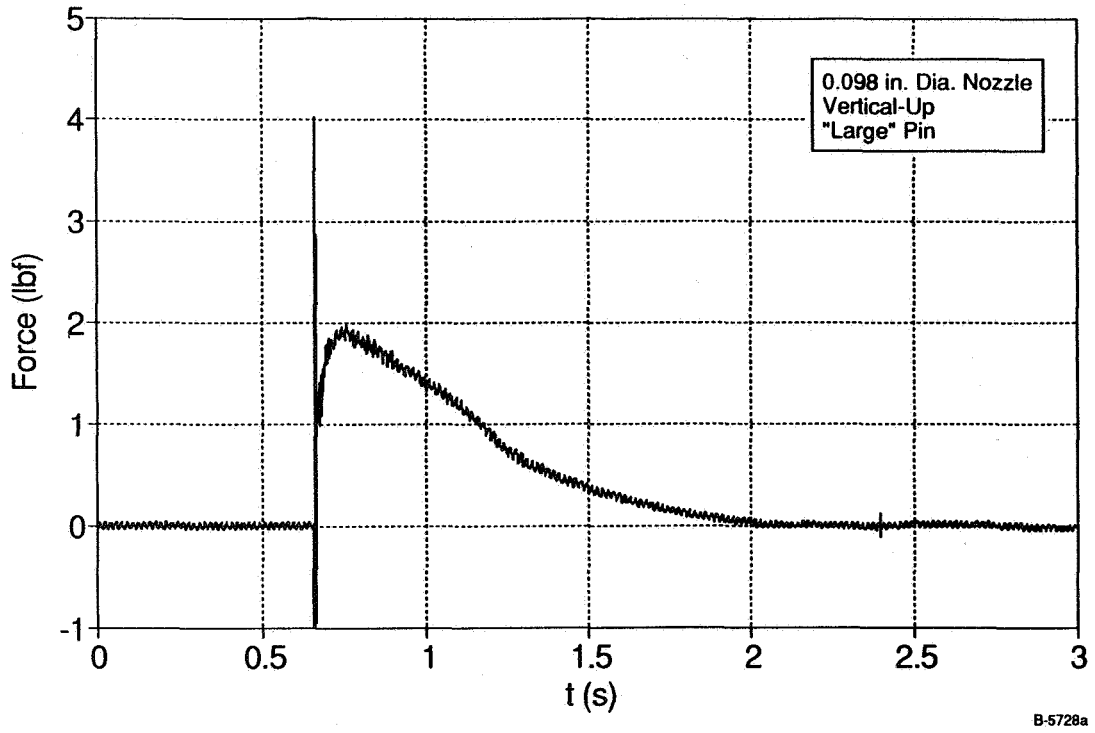


(a) Thrust versus Time

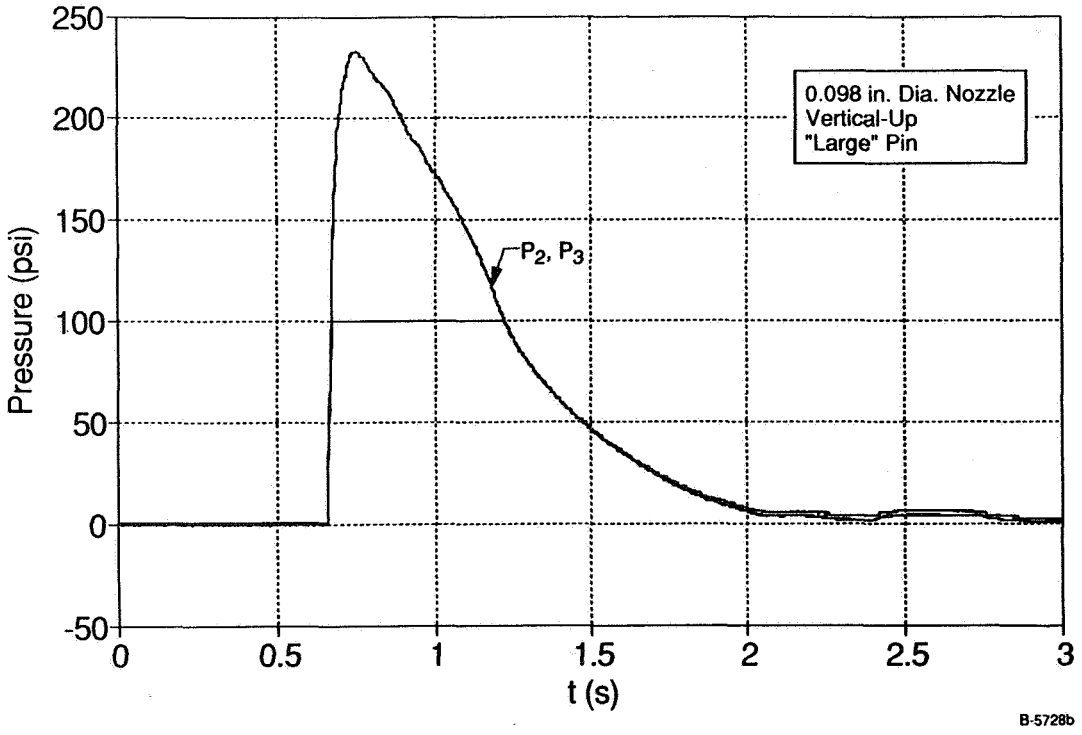


(b) Pressure versus Time

Figure 5. Thrust and Pressure Time History for Baseline Configuration Without Copper Plug (large pin, 0.098-in. diameter nozzle, vertical up orientation)

escapes through the nozzle. The thrust behavior correlates well with the pressure history in Figure 5(b). The pressures $P_2$ and $P_3$ are coincident in this figure. Unfortunately, the $P_1$ transducer was overpressurized and saturated during this run. The initial spike in Figure 4(a) is an ubiquitous feature of most thrust data. It represents the impact of the piercing pin on the diaphragm of the $CO_2$ cylinder. The duration of this spike is a few milliseconds. It should also be pointed out the time elapsed from the instant that the laser triggers the light-activated switch to the instant the pin impacts the cylinder is of the order of 20 to 50 ms. This interval includes the electronics reaction time and the firing of the squib.

Figure 6 shows thrust and pressure histories when three sets of copper plugs, each packed with 2 mm diameter copper spheres, are placed upstream of the nozzle. A comparison of Figures 5 and 6 shows that the thrust curves are nearly the same and the pressures are also substantially similar. Thus, for the simulator with a large (or standard) piercing pin, the copper plug has little effect on the flow and pressures inside the simulator.

Figures 7 and 8 show the effect of simulator orientation on thrust and pressure characteristics. In Figure 7, the simulator was horizontal and incorporated the same copper plugs as the configuration in Figure 6. The peak thrust in the horizontal orientation is slightly higher and falls off somewhat faster than the vertically up orientation of Figure 6. The data in Figure 7 is also more noisy and is believed to be an artifact of the simulator cantilevered from the load cell. The pressures in Figure 7(b) are seen to be greater than those in Figure 8(b), which explains the thrust behavior. Figure 8 shows data for the simulator firing the jet vertically down. The copper plugs are the same as for Figures 6 and 7. A comparison between Figure 6 and Figure 8 reveals that the thrust is substantially higher when liquid $CO_2$ is drawn because greater mass of $CO_2$ enters the stagnation chamber in a given time. Further, the thrust maintains its higher level for about 0.5s before beginning to drop-off rapidly. This behavior suggests that the liquid $CO_2$ escaping into the stagnation chamber of the simulator (Figure 2) vaporizes. During this process, liquid-vapor equilibrium is maintained, and the pressure tends to remain constant. However, the pressure drops as the $CO_2$ vapor leaves through the nozzle. The net effect of these two opposing processes is to reduce the rate at which pressure and thrust drop. A comparison of Figures 8(b) and 6(b) shows higher pressure for the vertically down orientation. Also, the behavior of pressure with respect to time in Figure 8(b) explains the thrust history in Figure 8(a).

During the series of static tests, visual observations of the $CO_2$ jet from the nozzle indicated presence of white mist frequently, even with the copper plugs and bronze wool in place. Thus the effectiveness of the copper spheres in vaporizing solid particles upon contact is questionable. It is possible that the particles are so fine that they follow the gas streamlines without actually making contact with the spheres.

It can be summarized from results of the small-scale simulator that a working device was developed for wind tunnel test in the University of Southampton MSBS. It was difficult to insure high degree of repeatability of thrust for several reasons. First, the tolerance on the thickness of the caps of the commercially available $CO_2$ cylinders was unknown. Secondly, the explosive capacity of the squibs was not uniform. These uncertainties made the mechanics of cap piercing not too repeatable. Furthermore, upon piercing the cap, the metallic piece of the material sometimes remained attached to the pin, restricting the mass flow through it. Also, as the pin wore out after repeated fixings, the piercing characteristics changed, contributing further to non-repeatability.

## 4. LARGE-SCALE PROPULSION SIMULATOR PRELIMINARY DESIGN

As mentioned earlier, the large-scale simulator design was based upon the lessons learned from the small-scale simulator experience. The large-scale device was intended only for static testing on a thrust stand. It is apparent from the review of the small-scale test data that a pressure control component and a means of vaporizing small solid $CO_2$ particles must be incorporated into the large-scale design. Furthermore,

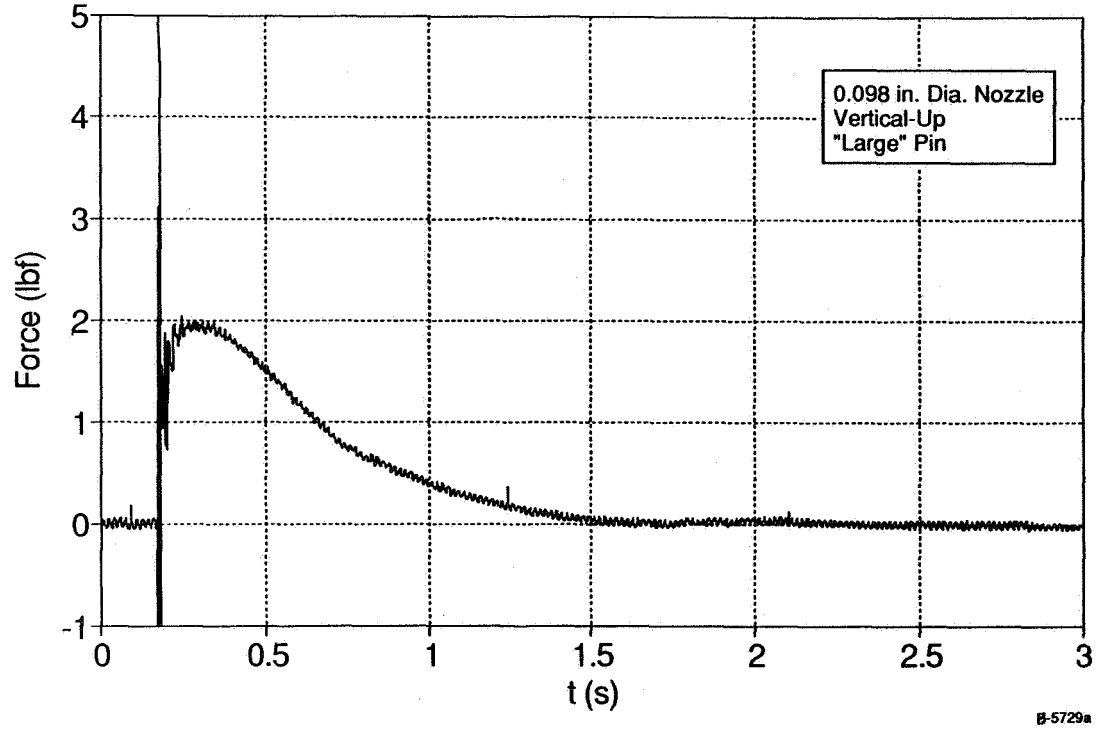


(a) Thrust versus Time

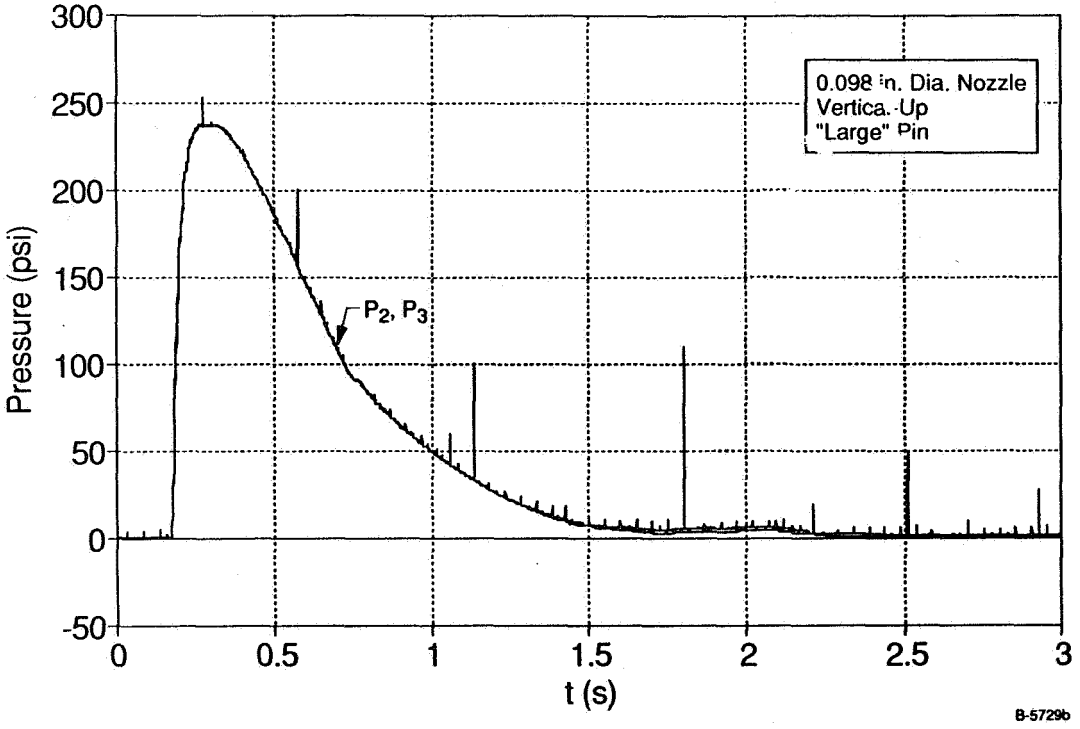


(b) Pressure versus Time

Figure 6. Effect of Three Sets of 2 mm Diameter Copper Spheres son Thrust and Pressure Time History (large pin, 0.098-in.diameter nozzle, vertical up simulator orientation)

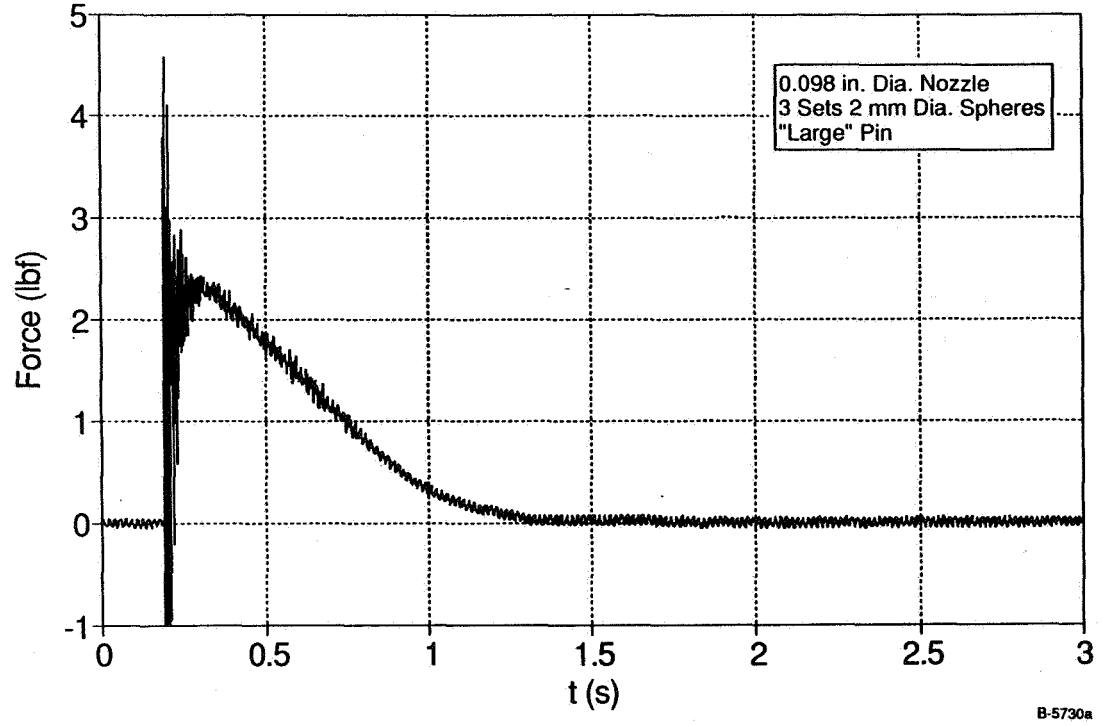


(a) Thrust versus Time

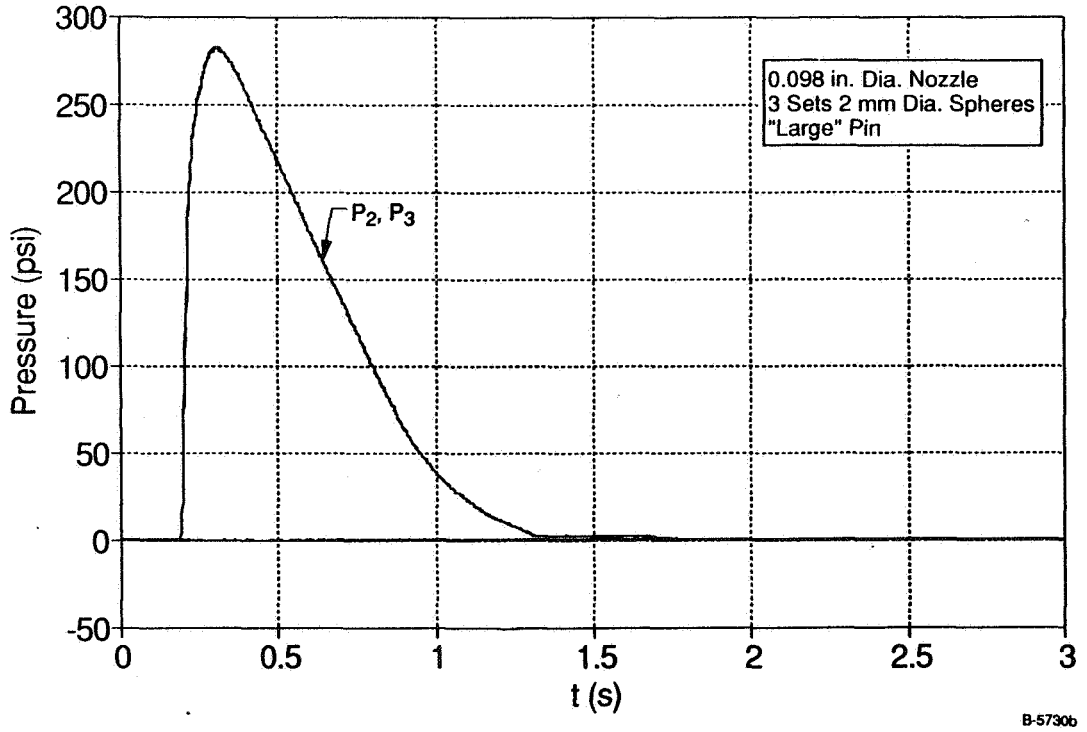


(b) Pressure versus Time

Figure 7. Effect of Horizontal Simulator Orientation on Thrust and Pressure Time History (large pin, 0.098-in.diameter nozzle, three sets of 2 mm copper spheres)

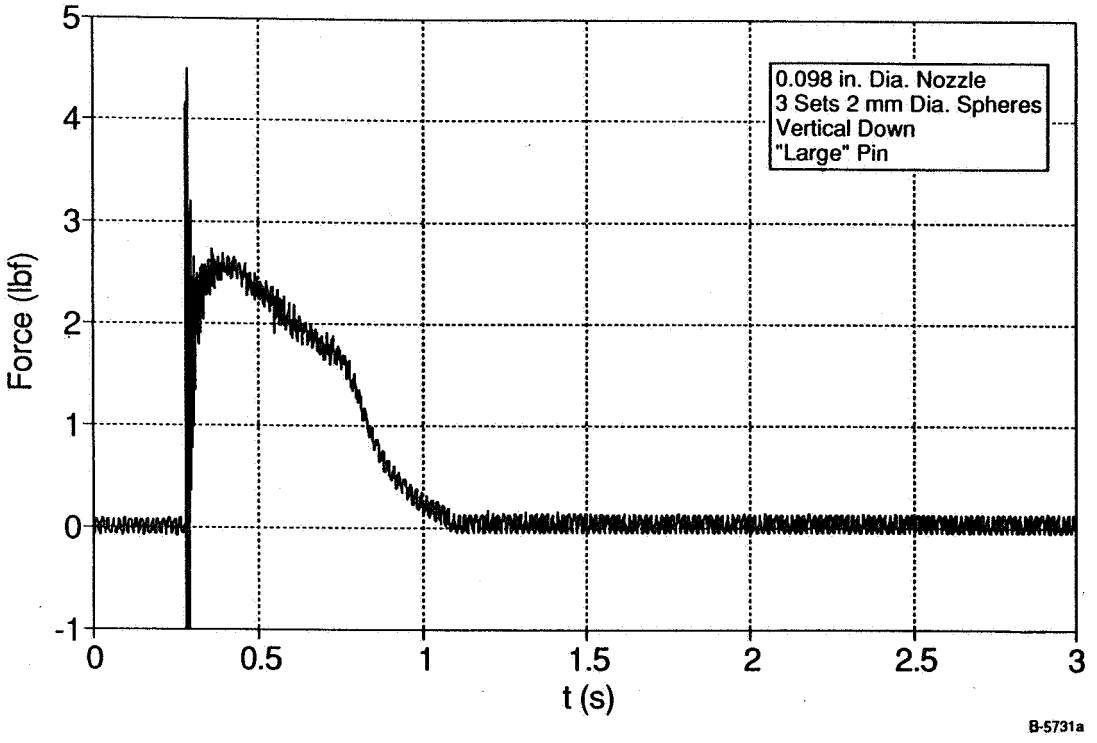


(a) Thrust versus Time

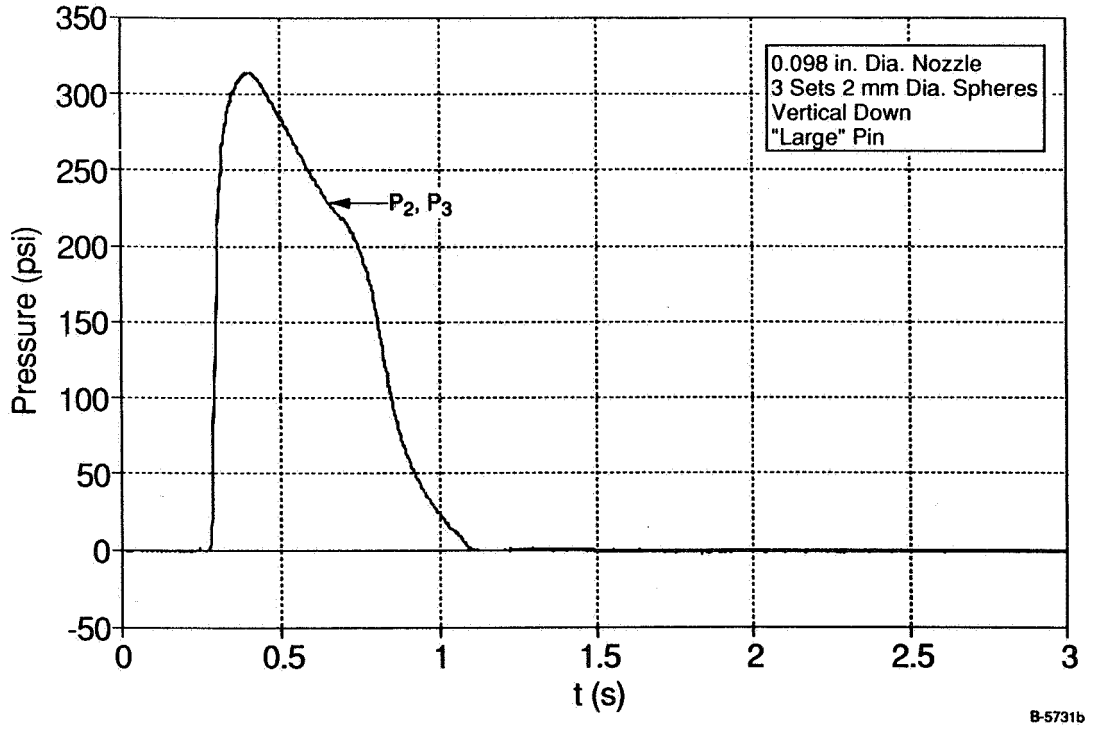


(b) Pressure versus Time

Figure 8. Effect of Vertical Down Simulator Orientation on Thrust and Pressure Time History (large pin, 0.098-in.diameter nozzle, three sets of 2 mm copper spheres)

one must be able to turn the simulator on/off during wind tunnel testing. The thrust and mass flow requirements are as defined in Ref. 1.

Taking the above requirements into account, the simulator design shown in Figure 9 was developed. The overall envelope is 2.5 in. dia. x 15 in. long. A copper reservoir holds about 200g of $CO_2$ when full, resulting in a total simulator weight of 5.5 Kg. Liquid, rather than vapor, carbon dioxide is drawn from the reservoir via an eductor tube to attain high mass flows ($\sim$40 g/s was achieved). The flow of liquid $CO_2$ is turned on/off by a miniature solenoid valve made by General Valve Corporation. It is operated by an on-board battery via a light-activated switch. $CO_2$ liquid flows through five coiled copper tubes which form a compact pre-heater block. It vaporizes and expands in the process, dropping its pressure. The pre-heater employs a cartridge heater which is run on external AC power prior to a propulsion test run. The power connector can be on the model on at the wall. It will be removed before a test run. The flow from the pre-heater enters a short settling/stagnation chamber and exits through a contoured nozzle. The nozzle was designed to be removable and replaceable. The pressure ratio was varied by varying the throat area.

As will be shown in Section 6, the simulator developed a thrust of 1.25 Kgf for approximately 4s. A maximum nozzle pressure ratio of 4.5 was attained.

The following paragraphs describe the main components of the large-scale simulator.

a) $CO_2$ Reservoir

The $CO_2$ reservoir, shown schematically in Figure 10(a), consists of a nickel-plated copper cylinder, 7 in. long, 2.5 in. O.D., 0.25 in. wall thickness; with a stainless steel plug threaded into its open end and sealed to the cylinder by a buna-N o-ring. The reservoir has a capacity of 200g of liquid $CO_2$. It was designed to withstand a pressure of 2000 psi, with a factor of safety of 4 to ultimate, and was proof-tested to 2500 psi. The copper cylinder has sufficient thermal mass to maintain the temperature, and therefore pressure, of the liquid $CO_2$ during the run. Furthermore, $\sqrt{\alpha t}$, i.e., the square root of the product of the thermal diffusivity of copper and the run time, equals

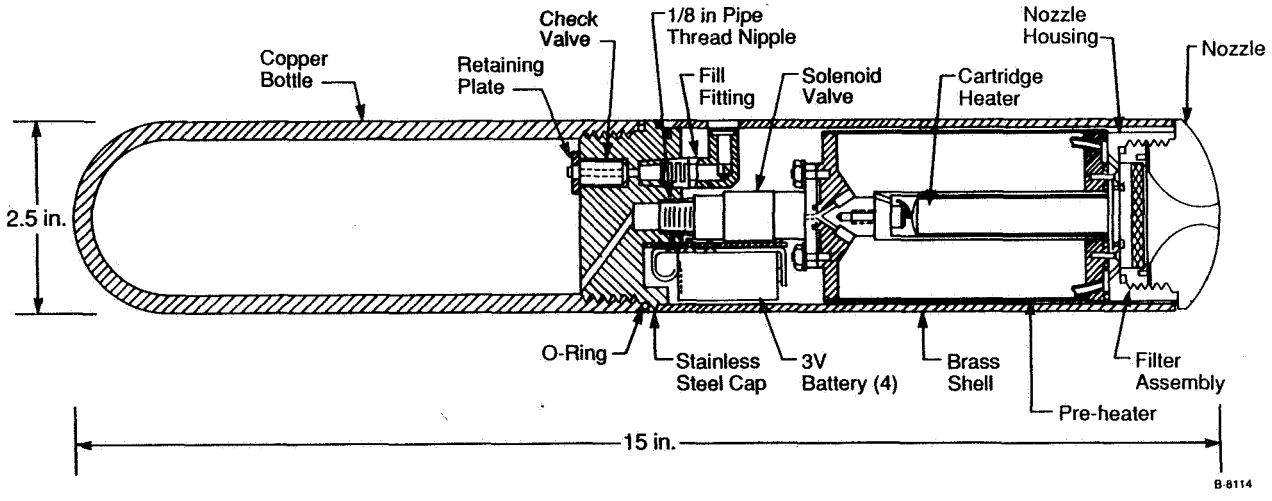


Figure 9. Design of Large-Scale Propulsion Simulator

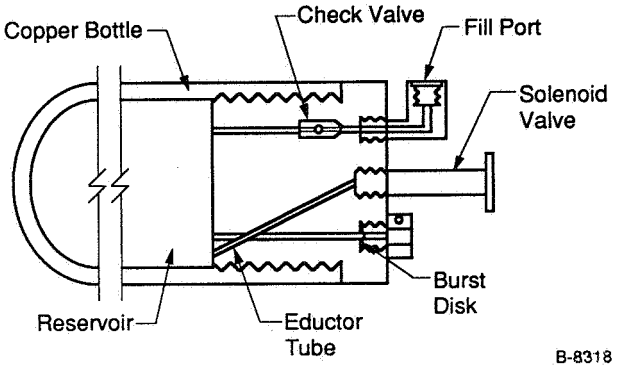


(a) $CO_2$ Reservoir

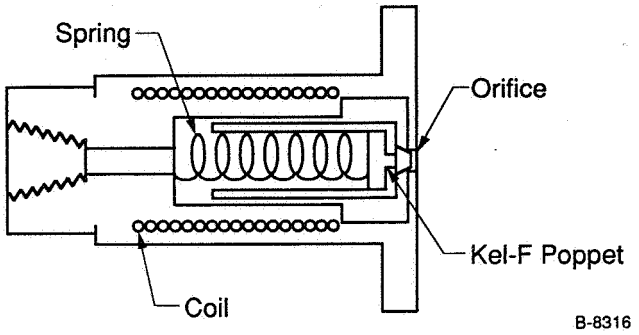


(b) Solenoid Valve

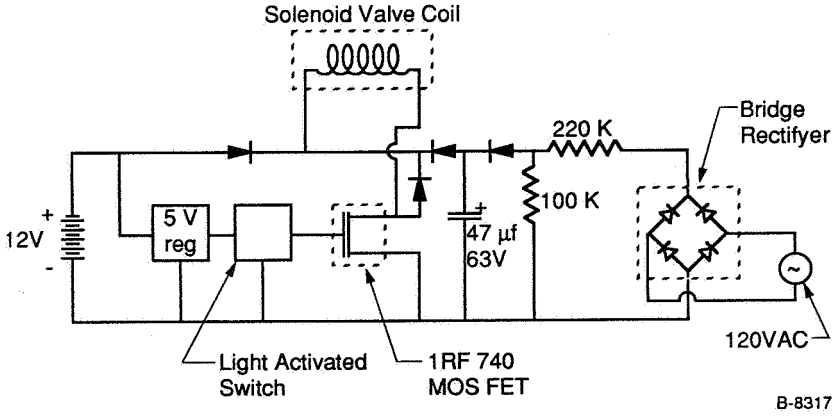


(c) Triggering Circuit

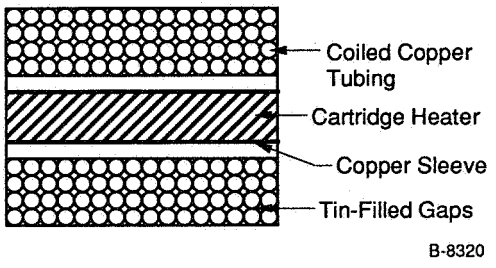


(d) Pre-heater/Pressure Reducer

Figure 10. Large-Scale Propulsion Simulator Components

2.1 cm, a factor of three greater than the wall thickness. Therefore, the $CO_2$ is able to draw heat from the entire thickness of the cylinder. The stainless steel cap contains a filling duct with a check valve (Kepner, 6000 psi max, 2 psi cracking); a burst disk (Frangible Disks, 1875 psi burst) to prevent over-pressurization; and a 0.093 in. dia. duct (eductor tube) to carry liquid $CO_2$ from the bottom of the cylinder to the solenoid valve.

b) Solenoid Valve

The solenoid valve, shown schematically in Figure 10(b), was manufactured by General Valve Corporation. Its dimensions are 1.6 in. long x 0.7 in. dia., and it weighs approximately 80g. It has a maximum operating pressure of 900 psi and is sealed by buna-N o-rings. The coil is rated for 6V and draws 2 amps during steady state operation. The valve operates by pulling a Kel-F poppet off of a 0.060 in. dia. orifice when the coil is activated. The valve is able to pass 40 g/s of liquid $CO_2$ through the orifice with an upstream pressure of 840 psig.

c) Triggering Circuit

The triggering circuit is shown in Figure 10(c). Basically, it consists of four 3V batteries in series with the valve coil, with power switched by an IRF740 MOSFET, which in turn is activated by an EG&G light activated switch. Twelve volts are used because during operation the coil draws enough current to drop the battery voltage to the rated voltage of 6V. Also in series with the coil is a 47 $\mu$f 63V electrolytic capacitor. Before each run, this capacitor is charged to 50V via external AC power and a bridge rectifier. (The capacitor charges in approximately 30s.) This capacitor sends an extra boost of current through the coil when the switch is first closed which helps to pull the valve open. Blocking diodes prevent communication between the capacitor and the batteries and prevent the capacitor from discharging to ground when AC power is removed. The light activated switch and a 5V regulator drain about 6 mA of current when the circuit is "off".

d) Pre-heater

After exiting the solenoid valve, the liquid $CO_2$ passes through a pre-heater to vaporize it and increase its enthalpy before entering the nozzle. The pre-heater transfers enough heat to the flow to increase its enthalpy by 180 kJ/kg, which is sufficient to prevent condensation when the $CO_2$ expands to 1 atm. It also drops the pressure of the flow to 70 psig in the nozzle chamber, although this pressure drop is a function of the mass flow (controlled by the solenoid valve) and the nozzle area, rather than the pre-heater characteristics. The pre-heater is shown schematically in Figure 10(d). It consists of five copper tubes (through which the $CO_2$ passes), each 90 in. long and 0.065 in. I.D., coiled around a copper sleeve into a 3 in. long x 2.25 in. dia. cylinder. The gaps between tubes were filled with tin to increase the thermal mass of the assembly and to increase the thermal conductivity between tubes. At the center of the copper sleeve is a 400W cartridge heater. The entire assembly weighs 1400g. Before each run, 120 VAC is applied to the cartridge heater which heats the pre-heater assembly to 75°C in 90s. During a 4s run of the simulator, the pre-heater cools to ~0°C. A one-dimensional flow and heat transfer model has been developed which predicts that at a mass flow rate of 40 g/s, the pre-heater will transfer 180 J/g to the flow. This prediction is entirely consistent with the observed temperature drop of the pre-heater.

e) $CO_2$ Filling

The $CO_2$ reservoir was filled with liquid $CO_2$ using the apparatus shown in Figure 11. A flex hose attached at one end to a $CO_2$ supply bottle was connected to the simulator via a fill fitting mated to the fill port of the simulator and a quick connect. The check valve in the reservoir cap

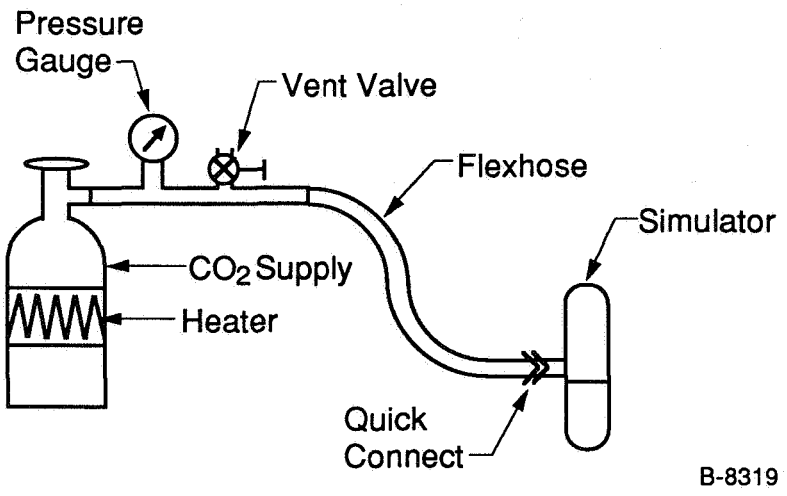


Figure 11. - $CO_2$ Filling Scheme

prevented backfilling. In order to fill the reservoir to a higher density of $CO_2$ than was in the supply bottle (without pumping), the reservoir had to be cooler than the supply. This necessitated either heating the supply bottle or cooling the simulator. We chose to heat the supply bottle (with heating tape) as this was quicker and easier than cooling the simulator and kept the simulator at room temperature. A thermistor was placed on the outside of the reservoir, and the density (and therefore mass) of the $CO_2$ in the reservoir was determined by measuring the temperature and pressure. This determination was verified by weighing the simulator before and after filling.

## 5. RESULTS OF STATIC TESTING OF LARGE-SCALE SIMULATOR

Figure 12 shows the schematic of the large-scale simulator static test stand. The objective of these tests was to demonstrate the repeatability of the thrust, multiple jet operation, and a reasonably flat thrust versus time profile. The measurements were thrust, pressure in the $CO_2$ reservoir, and pressure at the center of the nozzle exit plane, as a function of time.

Figure 13(a) shows typical static test data for the large-scale simulator. The thrust profile is essentially flat at 2.75 lbf (1.25 Kgf) for about 4s. The time required to attain 90 percent of full thrust is approximately 0.4s. The gradual drop-off is due to $CO_2$ vapor after all the liquid $CO_2$ has changed phase. Plotted in Figure 13(c) is the exit plane pressure on the nozzle centerline. These data have been corrected for the normal shock in front of the pitot tube in Figure 12. The shock occurs because the nozzle used in the test was supersonic with an area ratio of 1.19.

Both Figures 13(a) and 13(c) show an initial "bump" which lasts for about 1s. Corresponding to this, there is an increase in pressure of the $CO_2$ vapor in the reservoir, following a sharp initial drop as the

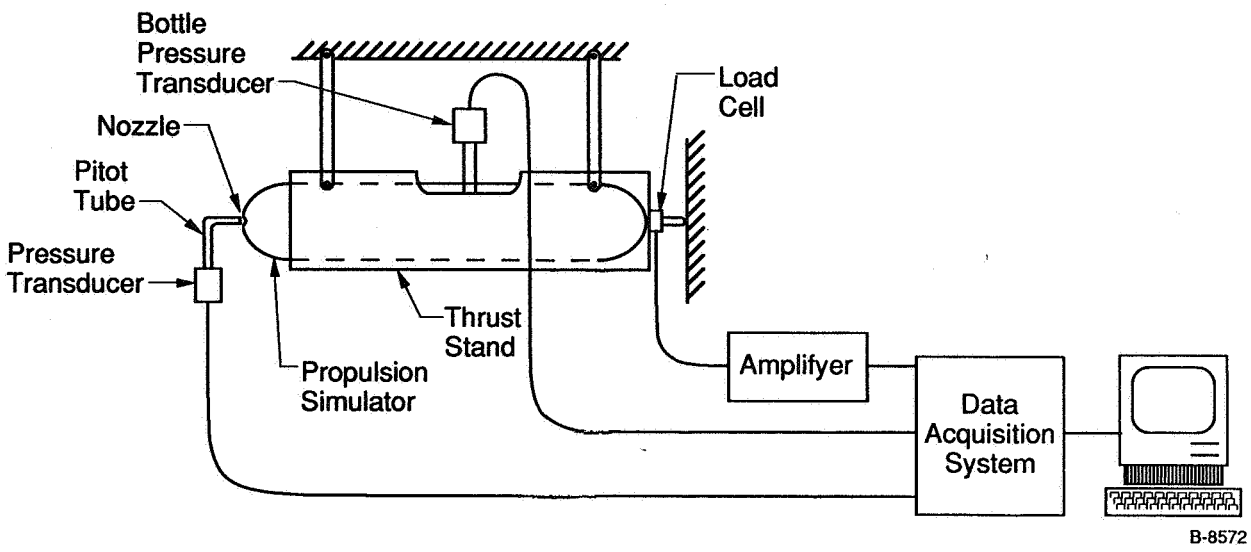


Figure 12. Schematic of Static Test Apparatus for Large-Scale Propulsion Simulator

solenoid valve is opened, Figure 13(b). The increase in pressure occurs as a result of the heat transfer from the copper wall of the reservoir to the $CO_2$ vapor. The sharp drop in pressure is believed to be due to "over-compression" of the $CO_2$ liquid during the filling process. It will be shown later in this section that slight under-filling of the reservoir avoids the initial sharp pressure drop and the subsequent bump in the thrust profile.

It is noted in Figure 13(b), that there is a distinct change in the slope of the $CO_2$ reservoir pressure curve after 5.5s. This is the point by which sufficient liquid has been drawn from the reservoir so that only vapor remains therein. As this vapor leaves the reservoir, the pressure drops rapidly, the mass flow rate through the system is significantly reduced, leading to a rapid drop in thrust as seen in Figure 13(a). Prior to t=5.5s, there is always some liquid inside the reservoir which continually vaporizes. As liquid $CO_2$ is drawn, the pressure and temperature of the vapor above it reduces. As heat is received from the copper walls, the temperature of the $CO_2$ liquid/vapor system rises, resulting in vaporization of the liquid. Ideally, this process should keep a constant pressure in the reservoir, provided the temperature of $CO_2$ system remains roughly constant. In reality, this does not happen, and the pressure does keep dropping between 1 and 5.5s, as seen from Figure 13(b). However, the rate of pressure drop is sufficiently slow that the thrust variations are small, as seen in Figure 13(a).

In Figure 14, the effect of under-filling the $CO_2$ reservoir on the thrust versus time curve is shown. It is seen from Figure 14(b) that the drop in $CO_2$ pressure upon activating the solenoid is much more gradual compared to over-filled case (Figure 13(b)). Also, there is no increase in the $CO_2$ pressure, unlike in Figure 13(b), following the initial drop in pressure. The result is that there is no bump in the thrust profile as was seen in Figure 13(a). This demonstrates that slight under-filling of the reservoir can produce a smoother thrust profile.

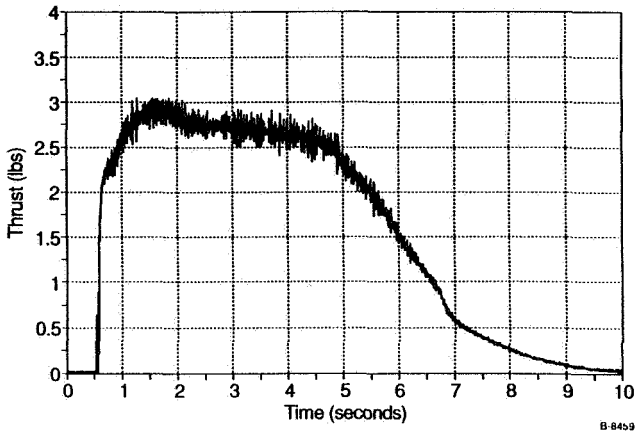


(a) Thrust versus Time

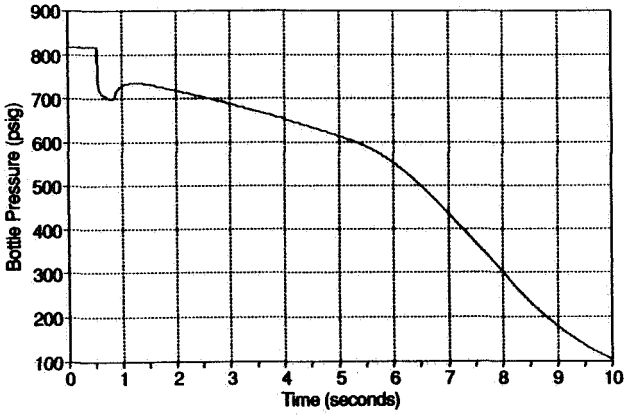


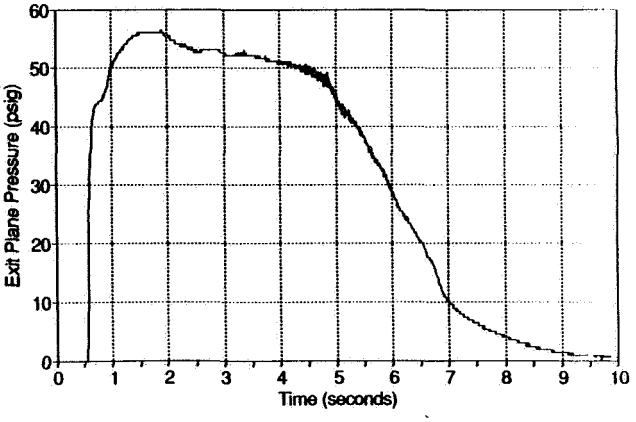


(b) Bottle Pressure versus Time

(c) Exit Phase Pressure versus Time

Figure 13. Large-Scale Simulator Static Test (Run 48)

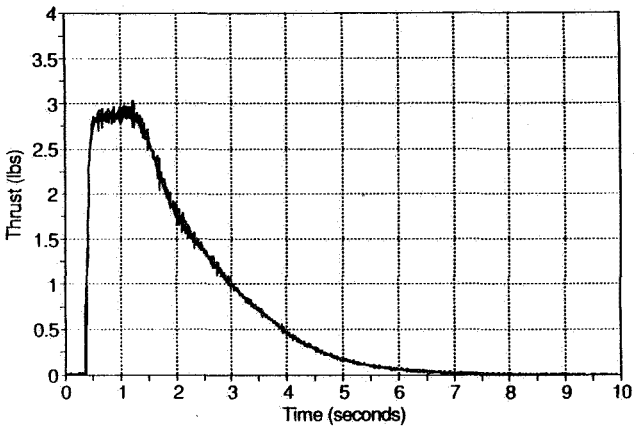


(a) Thrust versus Time

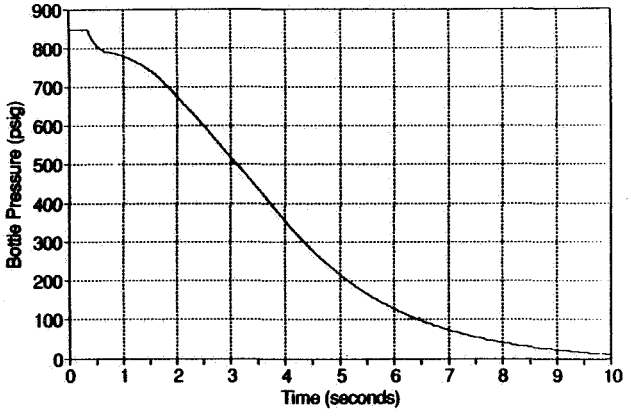


(b) Bottle Pressure versus Time

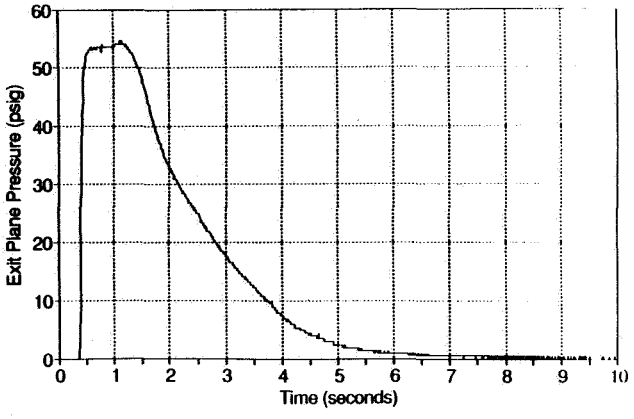


(c) Exit Phase Pressure versus Time

Figure 14. Effect of Under-Filling $CO_2$ Reservoir on Thrust Characteristics (Run 50)

Figure 15 shows the on/off capability of the large-scale simulator. This feature is necessary for producing jet pulses so that multiple runs can be made after filling the $CO_2$ reservoir. Note the absence of the bump in the thrust profile seen earlier for the over-filled reservoir.

An analysis of the thrust produced by the large-scale simulator is provided in Ref. 3. It is shown that the pressure ratio and thrust are directly proportional to the area of the flow orifice ($A_s$) of the solenoid. In the static tests, nozzle pressure ratio of the order of 4 to 5 were obtained (Figures 13(a) and 14(a), after accounting for the normal shock at the pitot tube). The pressure ratio can be lowered by increasing the nozzle throat area. The measured thrust of 1.25 Kgf is lower than the ideal thrust calculation (1.6 Kgf) given in Appendix D. The lower thrust (1.25 Kgf) and mass flow (40 g/s) when compared to the requirements of Appendix A (3 Kgf a 80 to 100 g/s), resulted from the flow restriction in the solenoid valve ($d_s$ = 0.060 in.). This particular valve, made by General Valve Co., was selected as an inexpensive, miniaturized device. In principle, a specially designed valve with a larger orifice can be incorporated in the current simulator design to yield the required 80 g/s mass flow. The current pre-heater can also handle mass flows of this magnitude.

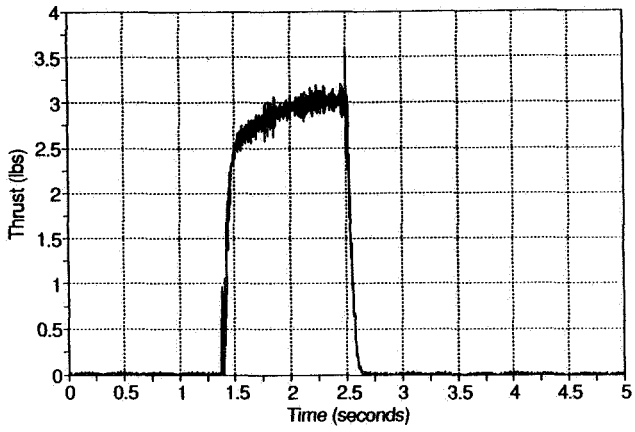


(a) Pulse 1

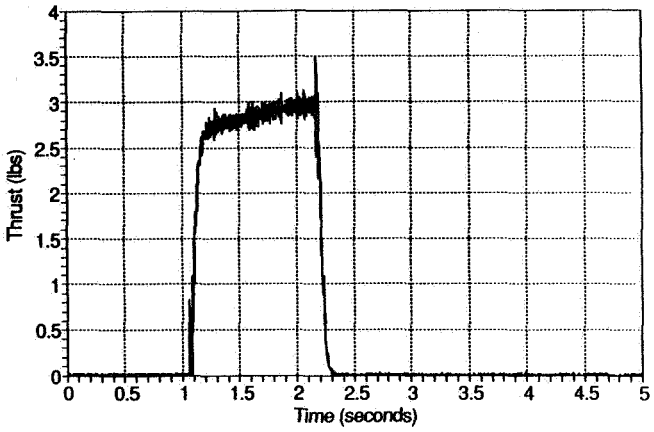


(b) Pulse 2

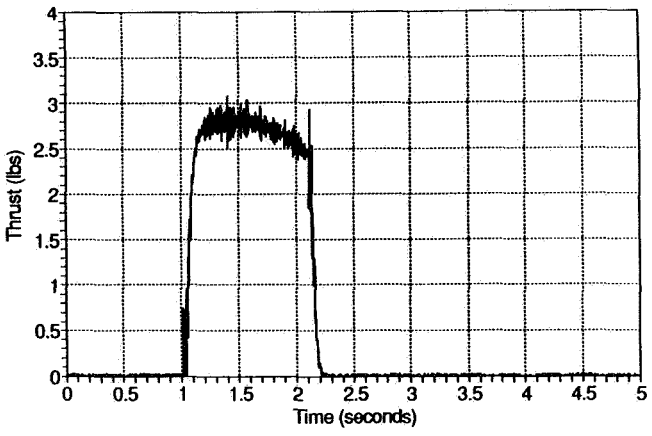


(c) Pulse 3

Figure 15. Multiple Run Operation of Large-Scale Simulator

## PART II

## UNIVERSITY OF SOUTHAMPTON MSBS MODIFICATIONS FOR PROPULSIVE TESTING

### 1. THE UNIVERSITY OF SOUTHAMPTON MSBS

In order to increase the versatility of the Magnetic Suspension and Balance System (MSBS) applied to the testing of wind tunnel models, development of techniques for simulation of propulsion systems is under way. The purpose of the work described in this paper was to begin to address the issue of developing exhaust flow simulators. The outcome was a set of simulators, two of which were brought to the stage of operating on board models levitated in a wind tunnel. The levitated model featured a supply of gas, discharged on command for a brief period to produce a jet exhausting at the rear.

The simulator development was carried out under NASA SBIR 87-1 whereby two styles of gas generator were developed. These were a carbon dioxide thruster with the gas stored under pressure as liquid $CO$ , and a rocket thruster using a solid propellant as the gas generator.

To enable suspension and testing of the propulsion simulators at the University of Southampton, a number of modifications were required to the suspension system, the wind tunnel hardware and to the control system.

The present electromagnet configuration is shown in Figure 16(a) '+' layout is used, symmetrical apart from the skew in the lateral electromagnets. This was introduced to provide a side force at high angles of attack. Position sensing is achieved via five linear photodiode arrays and a system of laser light sheets (ref. 4). A PDP11/84 computer is currently used for control of the MSBS. Dual-phase advance control algorithms with proportional and integral feedback are employed (ref. 5).

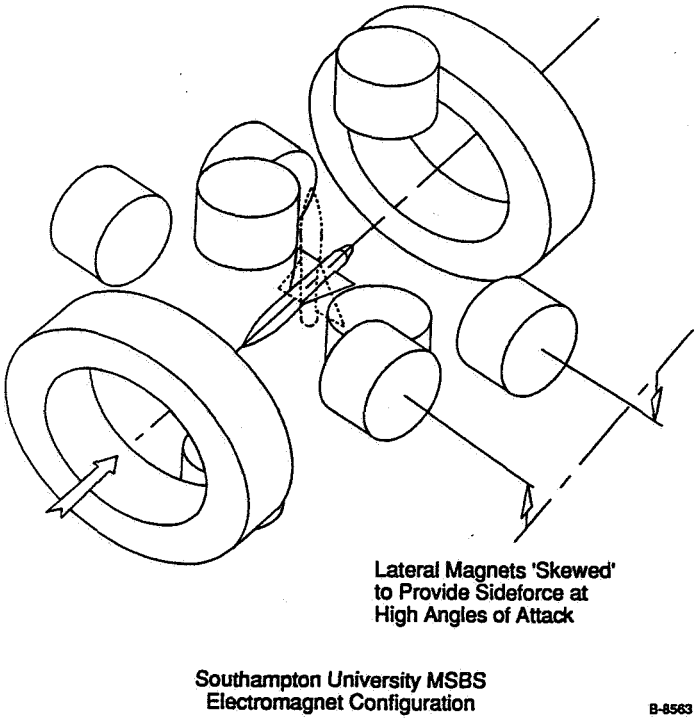


Figure 16. Electromagnetic Configuration for University of Southampton MSBS

The initial aim of the wind tunnel experiments was to test at speeds up to Mach 0.2, and at angles of attack up to twenty degrees.

## 2. SYSTEM MODIFICATIONS

It was necessary to alter the path of the axial position sensing laser light sheet, to avoid its corruption by the model's exhaust efflux. A change was made from tail to nose scanning, after consultation with PSI over a suitable nose geometry.

A PC was integrated into the control loop to act as a data logger, and eventual replacement for the PDP11 control computer. This allowed development of more sophisticated data analysis and presentation software than had previously been feasible at Southampton.

The high angle of attack control system was modified to allow suspension of iron models. It had originally been developed for use with models with permanent magnet cores. The change was necessary because machining the relatively complex components of propulsion simulators would have been very difficult with permanent magnet alloys. To magnetize the model a steady field component is added to the suspension field. The magnetizing field is generated by contributions from all ten electromagnets, and rotates to match the instantaneous angle of attack. The unique capability of the Southampton MSBS to suspend models over a 110 degree angle of attack range is thus retained.

It was found that a field strength of around 0.02 T was required to adequately magnetize the propulsion simulator, this rather high value being a result of its self-demagnetizing geometry. A number of additional minor system modifications were made.

## 3. INITIAL SUSPENSION AND DEVELOPMENT

Following initial suspension of the propulsion simulators, attempts were made to optimize the controller in each degree of freedom. Particular attention was paid to quality of suspension. Difficulties were expected in control of the simulators under the influence of force transients associated with the thruster firing. It was demonstrated that the optimum input constants to the dual-phase advancer were angle of attack dependent, rather than being constant for all angles of attack as had been previously assumed.

Further optimization was necessary to maximize the ability of the system to resist externally applied forces in the axial direction. This was achieved primarily by ensuring that the electromagnets used for axial force generation made the minimum practicable contribution to magnetization of the model. The level of magnetization was also adjusted to give the best compromise between strong magnetization and peak force generation.

Force and moment calibrations were performed to allow extraction of axial force data at zero angle of attack, and additionally for heave force and pitching moment data at angles up to twenty degrees. Conventional calibration techniques were employed, using small weights and low friction pulleys to apply forces to the suspended model, whilst recording the changes in electromagnet currents. Figure 17 shows the results of an axial force calibration, plotting magnet currents against externally applied load. The result is linear except at the extremes, where electromagnet current limits cause a non-linear region.

At zero degrees only the two axial magnets are used to oppose the drag force, so just their two currents are recorded during the calibration process. For other attitudes a technique was developed whereby several currents were recorded during heave, pitch and axial calibrations. Run-data was processed to find the changes in these currents during a suspended thruster firing, and matrix inversion used to deduce heave force, axial force and pitching moment simultaneously.

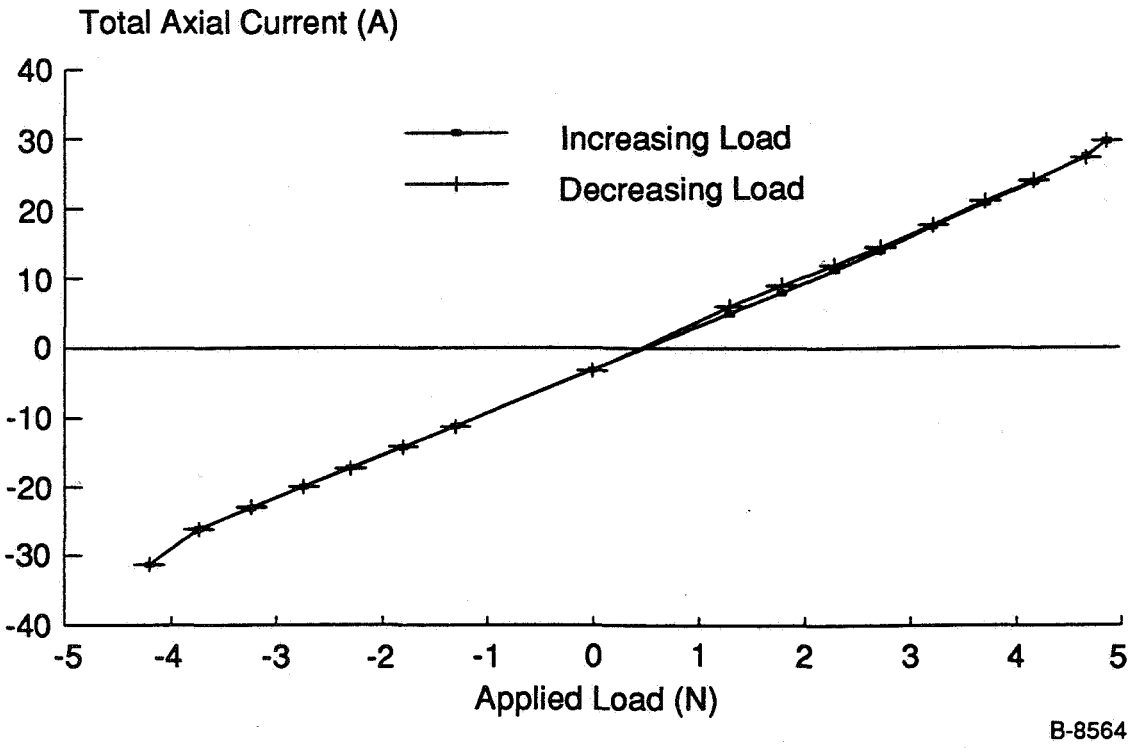


Figure 17. Axial Force Calibration at Zero Angle of Attack

Peak axial force capability was found to be around 4.5 N at zero angle of attack, falling to 4.0 N at twenty degrees.

Bench tests of the carbon dioxide thruster showed the peak thrust to be significantly above these values, and initial wind tunnel testing was delayed while a series of nozzle modifications gradually reduced the thrust peak to below 4 N. The rocket thruster used initially also displayed a thrust profile with an initial peak. In a later version the profile is more constant, as shown in Figure 18.

## 4. WIND TUNNEL TESTS

A series of firings of the carbon dioxide propulsion simulator was performed in the Southampton MSBS, at zero wind speed and up to Mach 0.1, and attitudes of zero, ten and twenty degrees angle of attack. Initially the success rate was only about 50%, with the model regularly falling out of suspension because of the high and erratic thrusts produced. Operating experience and further thrust reductions led to a much higher success rate. The rocket thruster has also been fired in suspension, and wind tunnel tests with this propulsion simulator will be performed in the near future.

## 5. DATA ANALYSIS AND RESULTS

The unsteady thrust profile and short run time of the carbon dioxide propulsion simulator provided particular problems for data analysis. As there was no period following a firing where the model was stationary during the thrust cycle, analysis of run-data had to address the motion transients. Software was developed to attempt to find the external forces and moments experienced by the suspended model, by considering its motion in addition to the electromagnet currents. Factors accounted for included the model's

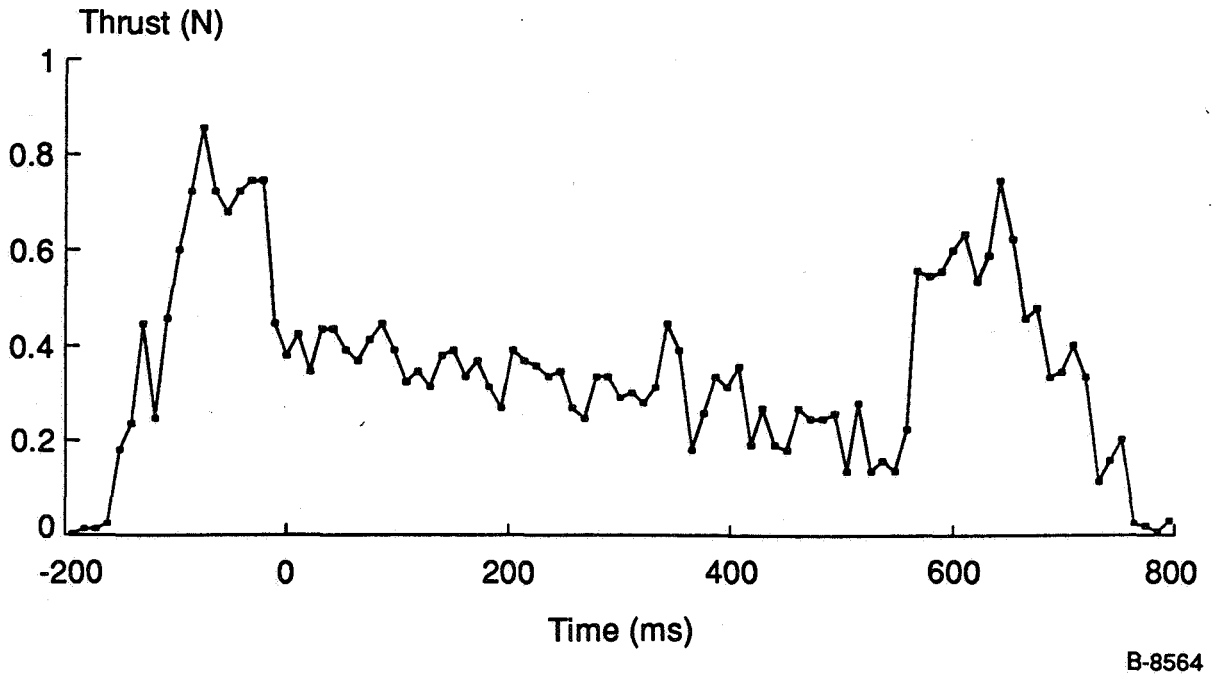


Figure 18. Rocket Motor Thrust Profile (low thrust test)

inertia, cross coupling in the position sensors, changes in level of magnetization and the relationship between calibration constant and axial position.

The aim was to extract a thrust profile similar to that demonstrated in bench tests, possibly going on to examine changes in drag coefficient caused by the presence of the exhaust plume. Unfortunately the variability of thrust produced by the carbon dioxide jet was such that no accurate measurements of this type were possible. In addition, the transient analysis did not prove satisfactory, giving external force data which did not agree closely enough with bench test results. In Figure 19, the bench test data shows an exponential thrust decay after the initial peak, while the data extracted from a test in suspension includes an oscillatory component, associated with model motion.

The force and moment results obtained with the model levitated were inconclusive. However the emphasis of the tests was placed on proof of concept and on overcoming some of the practical difficulties inherent in these experiments, rather than aiming to demonstrate an aerodynamic effect of the exhaust plume.

## 6. THRUST PROFILE AND MAGNETIC SUSPENSION

Control problems experienced using the PSI propulsion simulator were attributed to the very rapid increase in thrust to peak level when fired - the ramp lasting around 1 ms. Tests showed that the response to a demand for a step change in electromagnet current takes around 45 ms with the hardware presently in use at Southampton. The time measured to achieve peak restraining force during a suspended firing of the carbon dioxide thruster was also 45 ms, demonstrating a hardware, rather than a control software, limitation in responding to a sharply increasing thrust.

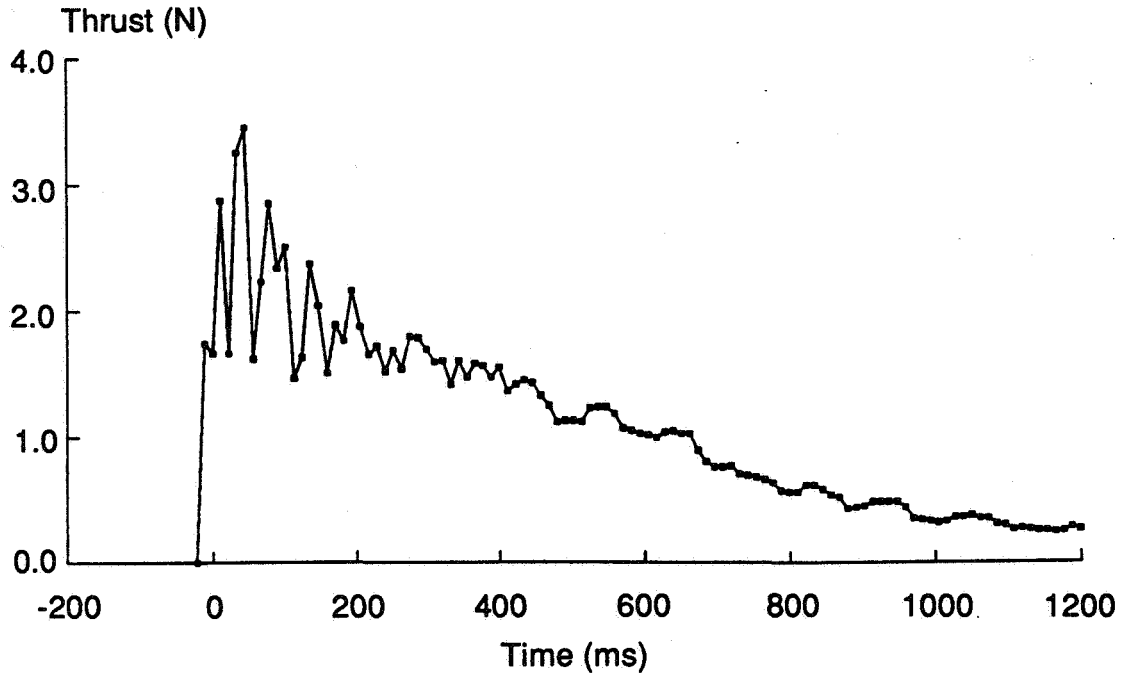


(a) Static Test Thrust Profile

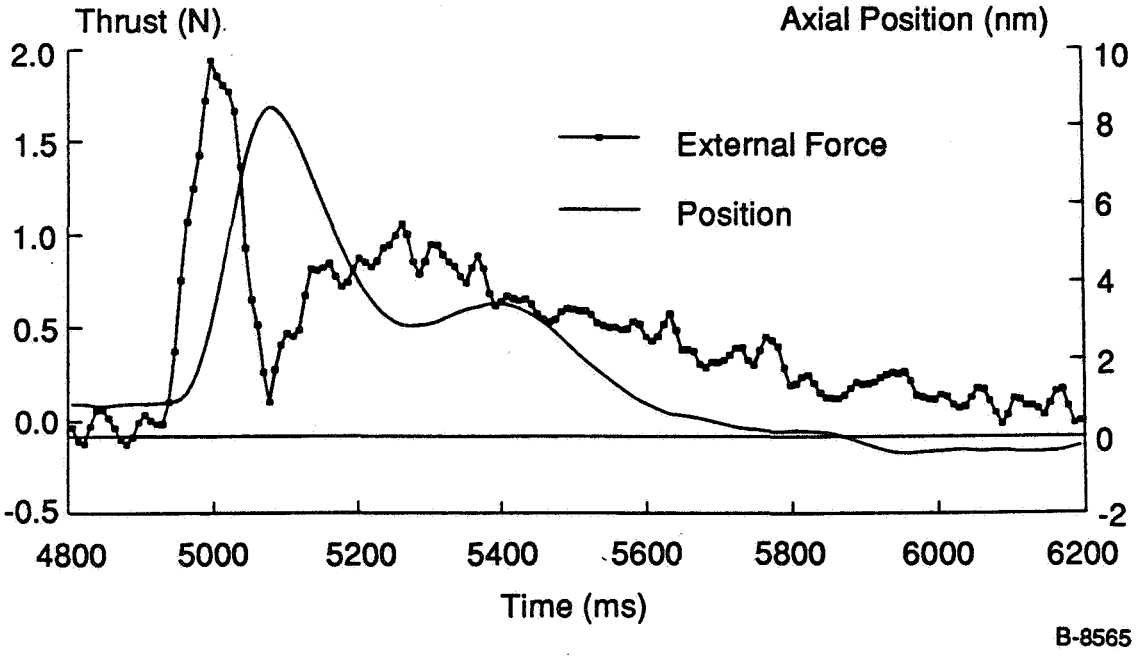


(b) Thrust Profile as Extracted from Current and Position Data

Figure 19. Measured and Extracted Thrust Profiles

Loss of control during firing was always preceded by excessive axial motion of the model, causing it to obscure the axial position sensor. A simple analysis showed that the lag between thruster firing and application of maximum restraining force made the amount of axial travel highly sensitive to variations in peak thrust. Results of this analysis are shown in Figure 20. For a low peak thrust the axial travel of the model is minimal. As the peak approaches the maximum restraining force the travel increases rapidly.

It is concluded that for reliable suspension during propulsion simulation in an MSBS, a thrust profile with a ramp to peak thrust of a similar time span to the minimum system response is necessary. Alternatively an unconventional model control system might be invoked.

The emphasis of this project was on proving that a model which carried a substantial thruster (peak thrust close to model weight) could be flown, fired and retained in controlled suspension. This aim was satisfied. It remains to develop the equipment and analysis further to the point where accurate force measurement is possible.

## 7. RESULTS AND CONCLUSIONS

The applicability of a wind tunnel employing Magnetic Suspension and Balance System (MSBS) to propulsive testing was demonstrated.

A small-scale propulsive device (1 in. dia. x 8 in. long), which generated a carbon dioxide jet, was designed, built, and statically tested to measure its thrust characteristics. It was successfully tested in the University of Southampton MSBS at angles-of-attack up to 20 deg.

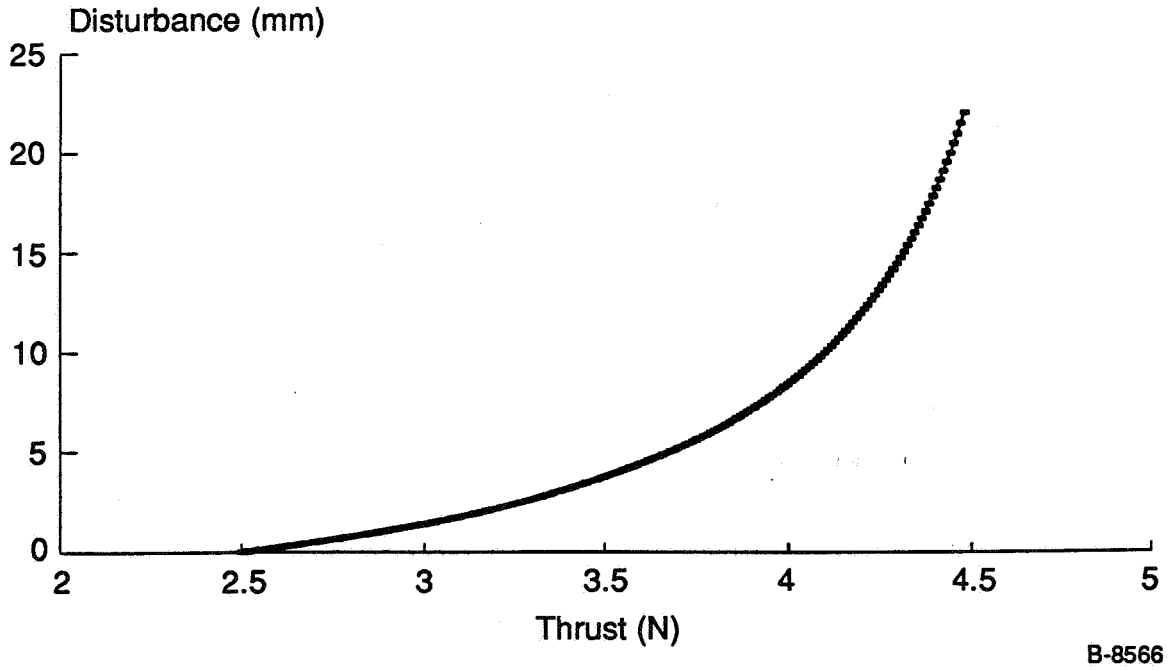


Figure 20. Results of Simplified Prediction of Model Response to Different Step Thrust Impulses

- The MSBS at Southampton was modified to keep the model stable under the action of the impulsive force generated by a thrusting model.

A large-scale propulsive device (2.5 in. dia. x 8 in. long), which generated a carbon dioxide jet, was designed, built, and statically tested to measure its thrust characteristic.

- A stable flat thrust profile was obtained over a period of 4s.

- Nozzle pressure ratios (NPR) of up to 5 were obtained. The device allows variation of NPR by varying the nozzle throat area.

- The propulsion simulator was demonstrated to operate in a pulse mode via a miniaturized solenoid valve.

- The thrust and mass flow of the current design are limited by the largest orifice (0.060 in. dia.) in the commercially available miniature solenoid valve. This limitation can be removed by using a specially designed miniature solenoid valve.

## 8. RECOMMENDATIONS FOR FUTURE PROPULSION SIMULATOR WORK

The present work has developed a propulsive device which can generate an exhaust jet with appropriate characteristics, such as thrust, mass flow, and pressure ratio. Although the initial motivation for this work was application to magnetic suspension, the propulsion simulators can be employed in conventional wind tunnel test applications as well. In fact, conventional testing has less stringent requirements. For example, the electronics can be located external to the simulator, pre-heater can stay on continuously, etc. In particular, with the following modifications, the large-scale device can be made highly useful for conventional applications.

- Modify solenoid for larger mass flows
  - Increase orifice diameter to $\geq 2$ mm
  - Modify coil to overcome greater force
  - Recharge capacitor to higher voltage

- Operational changes
  - Automatic shut off for pre-heater
  - Power on during run

- Develop model of thermo-fluid dynamics of the simulator to understand transients and to improve short pulse operation.

The small-scale simulator developed in the current program is especially suitable for high-speed (supersonic), blow down testing. The device is compact so that it can be easily incorporated into a high-speed model; and its short thrust time ($< 1$s) is compatible with blow down run times (typically few seconds). With the following modifications, the small-scale simulator can be adapted to high-speed testing.

- Replace off-the-shelf $CO_2$ cartridges by specially made copper bottle to store $> 16$g of $CO_2$ and for effective heat transfer to the vapor inside the bottle.

- Replace current filling pin/squib mechanism by General Valve Solenoid.

- Locate battery-plus-electronics external to the simulator, outside the test section or as a small module attached to the support.

- Use stack of pre-heated copper balls to avoid condensation with the above modifications, it appears possible to package the simulator in an envelope 1.25 in. dia. x 10 in. long.

## 9. REFERENCES


1. Joshi, P.B., et al., "Propulsion Simulation for Magnetically-Suspended Wind Tunnel Models," Physical Sciences Inc., PSI-2055/TR-859, NASA Contract No. NAS1-18616, September 1988.

2. Tuttle, M.H., Kilgore, R.A., and Boyden, R.P., "Magnetic Suspension and Balance Systems, A Selected, Annotated, Bibliography," NASA TM 84661, July 1983.

3. Joshi, P.B., et al., "Propulsion Simulator for Magnetically-Suspended Wind Tunnel Models," PSI-2090/TR-1140, NASA Contract NAS1-18845, September 1991.

4. Parker, D.H., "Techniques For Extreme Attitude Suspension of a Wind Tunnel Model in a Magnetic Suspension and Balance System. University of Southampton Ph.D. Thesis, April 1989.

5. Britcher, C.P., "The Southampton University Magnetic Suspension and Balance System - a Partial User Guide. AASU Memo 83/8, April 1984.


## ACKNOWLEDGEMENTS


This work was supported by NASA Langley Research Center under Contract No. NAS1-18845. The authors wish to acknowledge the comments and contributions of Dr. Evan Pugh at Physical Sciences Inc. during this investigation.